Journal of Applied Pharmaceutical Science Vol. 13(09), pp 037-047, September, 2023
Available online at http://www.japsonline.com
DOI: 10.7324/JAPS.2023.6683
ISSN 2231-3354

HPLC fingerprinting/GC-MS analysis, and efficacy of *Hypericum perforatum* against cisplatin-induced hepato-renal toxicity in mice with insights into the TXNIP/NLRP3 pathway

Maha Badr Salem[1], Eman Adallah Morsi[2], Eman Ahmed El-Wakil[2], Naglaa Mohamed El-Lakkany[1], Tarek Abou-shousha[3], Heba Abdel-Hady[2*]

[1]Pharmacology Department, Theodor Bilharz Research Institute, Giza, Egypt.
[2]Medicinal Chemistry Department, Theodor Bilharz Research Institute, Giza, Egypt.
[3]Pathology Department, Theodor Bilharz Research Institute, Giza, Egypt.

ARTICLE INFO

Received on: 29/03/2023
Accepted on: 24/06/2023
Available Online: 04/09/2023

Key words:
Hypericum perforatum, cisplatin, inflammasome pathway, oxidative stress, phenolic compounds.

ABSTRACT

Hypericum perforatum (HP) has antioxidant and anti-inflammatory characteristics. Nevertheless, its anti-inflammatory effects against hepato-renal injury have not been investigated. Therefore, this survey is designed to evaluate the prophylactic effect of HP extract against cisplatin- (CDDP-) induced hepato-renal toxicity in mice. Also, the active ingredients of HP were recognized. Hepato-renal toxicity was prompted by a single dose of CDDP (13 mg/kg, intraperitoneally). HP was tested at 50, 100, and 200 mg/kg/day for 10 days. Liver and kidney enzymes, oxidative stress, and inflammatory markers were examined, and histopathological examinations were performed. Total phenolic and flavonoid contents, besides 2,2-diphenyl-l-picrylhydrazyl radical scavenging activity, were assessed by identifying HP chemical compounds through high-performance liquid chromatography (HPLC) fingerprinting and gas chromatography-mass spectrometry. HP at 200 mg/kg improved hepatic and renal biochemical markers, reduced oxidative stress, and restored normal liver and kidney histology. Moreover, HP reduced inflammation by inhibiting TXNIP and NLRP3 tissue contents and cleaved caspase-1, interleukin-1β, and nuclear factor kappa-β expressions. The HPLC fingerprinting revealed high concentrations of ellagic acids, cinnamic acids, quercetin, and hesperidin, which may be responsible for alleviating hepato-renal damage. HP is an effective therapeutic agent against CDDP-induced hepato-renal toxicity and could be a realistic adjuvant therapy with CDDP for cancer treatment.

INTRODUCTION

Cisplatin (CDDP) is a chemotherapy medicine that is used to cure a wide range of malignancies. Despite CDDP being essential for cancer treatment, it is linked to severe toxicity in important organs, with the liver and kidneys being the most severely impacted (Sallam *et al*., 2021).

Although recent progress has been made in identifying the pathways implicated in CDDP-induced kidney and liver injury, mechanisms remain unknown. Reactive oxygen species, suppression of antioxidant enzymes, and lipid membrane peroxidation are some postulated mechanisms of CDDP-induced toxicity (Dasari and Tchounwou, 2014). It also activates numerous signaling molecules, including nuclear factor kappa-β (NF-kβ), which adjusts the activation of proinflammatory cytokines like interleukin-1β (IL-1β) (Wu *et al*., 2018).

The NOD-like receptor family, pyrin domain-containing protein 3 (NLRP3) inflammasome, is a multiprotein complex consisting of NLRP3, adaptor apoptosis-associated speck-like protein, and procaspase-1. TXNIP, an endogenous thioredoxin antagonist, and NLRP3 perform essential roles in the genesis and

*Corresponding Author
Heba Abdel-Hady, Medicinal Chemistry Department, Theodor Bilharz Research Institute, Giza, Egypt.
E-mail: h_hady10 @ yahoo.com

progression of kidney and liver illnesses (Molyvdas *et al*., 2018; Wu *et al*., 2018) TXNIP triggers caspase-1, which is accountable for the exchange of pro-IL-1β for mature IL-1β, which elicits severe inflammation through receptor activation. Two different pathways are included in synthesizing mature IL-1β (Aranda-Rivera *et al*., 2022). NF-kβ signaling produces pro-IL-1β, which is then cleaved by caspase-1 to produce mature IL-1β (Anders and Muruve, 2011).

Because of CDDP's high potency, it cannot be avoided in recent anticancer therapy. Despite significant CDDP toxicity, novel medicines to overcome the systemic side effects of CDDP therapy are urgently needed. Owing to their outstanding antioxidant and anti-inflammatory activities, natural products are acknowledged as a promising method to prevent CDDP-induced damage (Sioud *et al*., 2021).

Hypericum perforatum L. (Hypericaceae) (HP), a perennial plant often known as St. John's wort, has a long history in traditional medicine that dates to ancient Greek and Europe (Pardo-de-Santayana *et al*., 2015). HP was considered to be safe due to its nontoxic impact, which has been recorded at doses ranging from 100 mg/kg to 9 g/kg for different extracts (Arokiyaraj *et al*., 2011; Sologub and Grytsyk, 2013). Truly, it has become conspicuous worldwide in treating depression and is a promising alternative to synthetic antidepressants (Kumar *et al*., 2010). Nowadays, it is requested in therapy for treating gastrointestinal syndromes and is recognized for its anti-inflammatory and antioxidant agent (Güzel *et al*., 2019; Napoli *et al*., 2018). Besides, HP contains secondary metabolites, including flavonoids (rutin, quercetin, hyperoside, etc.), phenolic acids (ferulic acid, caffeic acid, cinnamic acid, etc.), anthraquinone derivatives, tannins, and other water-soluble compounds (Greeson *et al*., 2001).

To the best of our knowledge, no former research has looked into HP's hepato-renal protective effects against CDDP-intoxication. This study aims to examine the protective role of HP administration on CDDP-induced hepato-renal damage in mice, emphasizing oxidative stress and inflammasome-related pathways. Phytochemical characterization of HP was also performed using high-performance liquid chromatography (HPLC) fingerprinting and gas chromatography-mass spectrometry (GC-MS).

MATERIALS AND METHODS

Gathering and identification of the plant

HP was obtained from Saudi Arabia in June 2020. Taxonomic identification of the plant was confirmed by Dr. Eman Karakish, Ass. Prof. of Plant Taxonomy, Faculty of Science, Ain Shams University, Egypt. The leaves were dried and then powdered, and the specimen was kept in the Medicinal Chemistry Department, Theodor Bilharz Research Institute (TBRI), Giza, Egypt.

Preparation of plant extract

The dried plant (500 g) was extracted with 85% methanol (MeOH) for 1 week. The extract was filtered and evaporated under a vacuum using a rotary evaporator (BUCHI) till dry. The crude extract was kept for further studies.

Preliminary phytochemical screening

Phytochemical screening for the main bioactive constituents of HP leaves was performed as previously described (Abdel-Hady *et al*., 2019; El-Wakil *et al*., 2019).

Total phenolic content

The phenolic content of the MeOH extract of HP leaves was studied using a spectrophotometric technique (Singleton *et al*., 1999). The total phenolic content was shown in milligram gallic acid equivalent (GAE) per gram dry weight of the extract (mg GAE/g dry extract).

Total flavonoid content

The content of flavonoids in the MeOH extract of HP leaves was determined using a colorimetric assay (Hady *et al*., 2018; Zhishen *et al*., 1999). The total flavonoid content was expressed as mg rutin equivalents (RE) per gram of extract (mg RE/g of extract).

2,2-diphenyl-l-picrylhydrazyl (DPPH) radical scavenging activity

The antioxidant potential of the tested extract was evaluated by the DPPH free radical scavenging method (Brand-Williams *et al*., 1995). Ascorbic acid was used as a standard.

Animals

Swiss albino mice (male), weighing 20–30 g, were provided by the animal house of TBRI, Giza, Egypt. Mice were housed in cages and fed with a standard pelleted diet and water *ad libitum*. Animals were kept in controlled environmental conditions at temperature (25°C ± 2°C) and humidity (50% ± 15%) under 12 hours of light/dark cycles. All the investigations were accepted by the Institutional Review Board of TBRI (PT 613, 28 June 2021; FWA 0010609).

Experimental design

Thirty-six mice were casually divided into six groups (six/group), as follows: group I: normal mice were given saline only once daily; group II: normal mice received oral dose (200 mg/kg daily) of HP; group III: mice received a single intraperitoneal injection (IP) dose of CDDP (13 mg/kg) (Domitrović *et al*., 2013) on the fifth day of the experiment; groups IV–VI: mice received oral doses (50, 100, and 200 mg/kg daily) of HP (Arokiyaraj *et al*., 2011), respectively, and received a single IP dose of CDDP (13 mg/kg) on the fifth day of the experiment. The initial and final body weight of each animal was recorded. After 10 days of treatments, mice were euthanized under anesthesia with thiopental (50 mg/kg, i.p.). Their livers and kidneys were removed and weighed, and their relative weight was calculated: (the organ wt. /body wt.) × 100.

Blood samples were centrifuged, and the sera were stored for biochemical analysis. The liver and kidney parts were homogenized in ice-cold saline to prepare a 10% homogenate for enzyme-linked imunosorbent assay (ELISA) measurements, while the other was used for histopathological examination. The protein content of tissue homogenates was determined (Lowry, 1951).

Assessment of liver, kidney, and oxidative stress biomarkers

Alanine aminotransferase (ALT), aspartate aminotransferase (AST), alkaline phosphatase (ALP), urea, and creatinine, as well as hepatic and renal glutathione (GSH) and malondialdehyde (MDA) levels, were measured using commercial kits (Biodiagnostic Co., Egypt) according to the manufacturer's instructions.

Enzyme-linked immunosorbent assay for TXNIP and NLRP3

Tissue content for TXNIP and NLRP3 as inflammatory markers was determined using ELISA kits (Sunlong Biotech Co., Ltd., China) according to the manufacturer's instructions, and the results were mentioned as pg/mg protein.

Quantitative real-time polymerase chain reaction (PCR) of cleaved caspase-1, IL-1β, and NF-kβ expressions

Total RNA was extracted from liver and kidney tissues by an RNeasy Mini Kit (Qiagen, Germany). The RNA quantity and purity were evaluated using a NanoDrop 2000 spectrophotometer (Thermo Fisher Scientific, Wilmington, DE). RNA (1 µg) was reverse-transcribed by Quantiscript reverse transcriptase (QuantiTect Reverse Transcription Kit, Qiagen). The PCR reactions were done with a Rotor-Gene Q thermocycler (Qiagen) using SYBR Green PCR Master Mix (Qiagen). The thermal cycling conditions were as follows: 3 minutes at 95°C, 40 cycles at 95°C for 10 seconds, the primer sequence and annealing temperatures listed in Table 1, and 72°C step for 30 seconds. Relative expression was calculated using the comparative cycle threshold (C_t) ($2^{-\Delta\Delta CT}$) method (Livak and Schmittgen, 2001).

Histopathological examinations

Parts of the liver and kidney were immediately fixed in 10% formalin. Samples were sliced into 5-µm-thick sections and stained with hematoxylin and eosin (H&E) for histopathological examination.

HPLC fingerprint analysis

Analysis of phenolic and flavonoids compositions was performed using HPLC apparatus (Agilent Series 1100, USA) composed of an autosampling injector, solvent degasser, two LC- pumps, with ChemStation software, and UV/VIS detector (set at 250 nm for phenolic acids and 360 nm for flavonoids). The analysis was achieved on a C18 column (125 × 4.60 mm, 5 µm particle size). Phenolic acids were detached using a gradient mobile phase consisting of two solvents: methanol and acetic acid in water (1:25) (Lin *et al*., 1996). Flavonoids were detached by using a mobile phase consisting of two solvents: acetonitrile and 0.2% (*v*/*v*) aqueous formic acid with an isocratic elution (70: 30) program (Kuntić *et al*., 2007). The injection volumes were set at 25 µl. Standard flavonoids and phenolic acids were prepared as 10 mg/50 ml in methanol, diluted to concentrations of 20–40 µg/ml. The major components present in the HP extract were quantified using peak area computation (external standard method) (El-Hawary *et al*., 2020).

GC-MS analysis

The crude MeOH extract was analyzed by the GC-MS method. It was done using a GC (Agilent Technologies 7890A) interfaced with a mass-selective detector (Agilent 7000) equipped with a polar Agilent HP-5ms (5%-phenyl methyl poly siloxane) capillary column (30 m × 0.25 mm i.d. and 0.25 Elm film thickness). The carrier gas was helium, with a linear velocity of 1 ml/minute. The injector and detector had temperatures of 200°C and 250°C, respectively: injection mode, split; split ratio 1:10, volume injected (1 µl). The ionization potential was 70 eV, the interface temperature was 250°C, and the acquisition mass range was m/z 50–600. The compounds were identified by comparing their mass spectra and retention time (RT) to those compounds, matching with the NIST and WILEY libraries.

Statistical analysis

Data are expressed as mean ± SEM. A one-way analysis of variance (ANOVA) test followed by least significant difference (LSD) *post hoc* test was carried out using SPSS, software package version 16.0 (Chicago, IL). p values < 0.05 were statistically significant.

RESULTS AND DISCUSSION

Preliminary phytochemical screening

Phytochemical screening is critical in identifying novel sources for professional use in drug discovery (Asgharian and Ojani, 2017). In this investigation, phytochemical screening of MeOH extract of HP leaves demonstrated the existence of several classes of bioactive constituents in the plant, as shown in Table 2. The results exhibited that alkaloids, carbohydrates, phenolics, flavonoids, tannins, anthraquinones, and saponins are present, but steroids are not. These secondary metabolites are effective in preventing several diseases and have variable medicinal activities, such as anti-inflammatory and anticarcinogenic properties (Negi *et al*., 2011; Yadav *et al*., 2014). Flavonoids and phenolics have a wide zone of biological efficiencies due to their free radical scavenger ability, leading to the prevention and treatment of several diseases (Victor and Shaikh Hamed, 2014).

Table 1. The primmer sequence and annealing temperatures for quantitative real-time PCR.

Target gene (s)	Amplicon length (bp)	Primer sequence
cleaved caspase-1	198	Forward primer: 5′-GCGAAGCATACTTTCAGTTTC-3′ Reverse primer: 5′-TCTCCTTCAGGACCTTGTCG-3′
NF-kβ	78	Forward primer: 5′-CTGGTGGACACATACAGGAAGAC-3′ Reverse primer: 5′-ATAGGCACTGTCTTCTTTCACCTC-3′
IL-1β	72	Forward primer: 5′-GCTGCTACTCATTCACTGGCAA-3′ Reverse primer: 5′-TGCTGCTGGTGATTCTCTTGTA-3′
Beta actin	118	Forward primer: 5′-GGGAATGGGTCAGAAGGACT-3′ Reverse primer: 5′-CTTCTCCATGTCGTCCCAGT-3′

Total phenolic and flavonoid contents

Phenolic and flavonoid compounds exhibit a strong free radical scavenging activity and an inhibition activity on carcinogenesis and inflammation (Tohamy *et al*., 2016). The results demonstrated that HP has promising content for phenolics and flavonoids (Table 3). According to the literature, phenolics and flavonoids may be responsible for protection against oxidative stress along with other antioxidants such as enzymes and vitamins (Ersoy *et al*., 2020; Siangu *et al*., 2019).

DPPH radical scavenging activity

As shown in Table 3, the DPPH (IC_{50}) of HP was evaluated and exhibited strong antioxidant activity, and the extract displayed inhibitory percentage ranging from 11% to 100% at concentrations ranging (5–500 µg/ml) (Fig. 1), which may be due to its phenolic and flavonoid contents. In fact, plants produce several secondary metabolites with numerous mechanisms to reduce free radicals that play an essential role in disrupting essentially biological processes in our bodies (Asgharian and Ojani, 2017). From the previous reports, the ethanol extract of HP has a strong inhibitory percentage, which may be comparable to ascorbic acid (Mašković *et al*., 2011). Furthermore, the leaves of HP extracts have a higher inhibition percentage than the flowers (Asgharian and Ojani, 2017). According to some studies, the ethanol extract of HP has higher antioxidant activity than butylated hydroxytoluene as a standard antioxidant (Ersoy *et al*., 2020; Güzel *et al*., 2019).

Effect of HP on body weight and relative organs weight

Table 4 shows the impact of HP on body weight and relative organs weights. According to the data, there were no statistically significant variations among the groups' weights at the beginning and the end of the experiment. All doses of HP significantly reduced ($p < 0.05$) the weights of their kidneys and the relative organs weights compared with the CDDP-intoxicated group. However, there was an insignificant difference in liver weight after treatment with all doses of HP compared to the normal mice. Relative organ weight is used as a valid predictor of tissue damage (Kim *et al*., 2014). Herein, the considerable rise in the values of relative liver and kidney weights after CDDP exposure may reflect the development of inflammation and oxidative stress. A previous study demonstrated that a substantial rise in relative kidney weight may be due to CDDP-induced organ injury (Lin *et al*., 2018). Notably, the significant decrease of liver and kidney indices in treated groups with HP may show the prophylactic effect of this plant against CDDP-induced liver and kidney lesions. Our results were in accordance with a previous study that found the protective effect of *Garcinia kola* and *Withania somnifera* kept the organ-to-body weight ratio of mice from changing significantly (Adejor *et al*., 2017; Rashid *et al*., 2021).

Table 2. Qualitative phytochemical screening of MeOH extract of HP leaves.

Phytoconstituents	Test	Result
Alkaloids	Wanger's test	+
Carbohydrates	Molisch's test	+
Terpenoids	Salkowski's test	+
Phenolics	Phenol test	+
Flavonoids	Shinoda's test	+
Tannins	Ferric Chloride test	+
Anthraquinons	Borntrager's test	+
Steroids	Steroid test	−
Saponins	Froth test	+

Effect of HP on hepatic and renal function biomarkers

CDDP causes hepato-renal damage, as evidenced by the rise of liver and kidney biomarkers in our study (Fig. 2). When comparing CDDP-intoxicated mice to normal mice, CDDP injection significantly elevated ALT (88%), AST (167%), ALP (48%), urea (45%), and creatinine (63%). In addition, treatment of healthy mice with HP alone had no significant effect on these parameters. Treatment of CDDP-intoxicated mice with 50 and 100 mg/kg led to a substantial drop in liver enzymes (ALT, AST, and ALP) and renal parameters (urea and creatinine). Besides, 200 mg/kg HP demonstrated significant decreases in liver enzymes (ALT, AST, and ALP) by 2.36-, 2.45-, and 2.61-fold, respectively, and renal parameters (urea and creatinine) by 2.11- and 2.91-fold, respectively, compared to the CDDP-intoxicated group. These detrimental effects on the liver and kidney are due to CDDP metabolism in hepatocytes and renal cells, plus alterations in their membrane permeability, resulting in intracellular enzyme leakage into the bloodstream (Farid *et al*., 2021). Elevation of liver enzymes correlates with the degree of hepatocyte membrane injury (Sioud, 2021). The elevation in renal enzymes is due to the reduction in glomerular filtration rate caused by CDDP (Elsayed *et al*., 2021). CDDP's toxic effect is entirely consistent with previous studies (Abo-Elkomy *et al*., 2020; Elmaaty *et al*., 2020). Liver and kidney functions were improved by the administration of HP extract, so HP may effectively stabilize the cell membrane and prevent the leakage of intracellular enzymes, preserving cellular functions. This may be owing to the antioxidant activity of HP and its bioactive constituents (Caglar *et al*., 2019; Zou *et al*., 2004).

Effect of HP on hepatic and renal oxidative damage parameters

The present study looked at oxidative stress markers (GSH and MDA) in the liver and kidney tissues of mice given CDDP. GSH levels in the liver and kidneys were considerably reduced by 34.49% and 43.62%, respectively. Furthermore, CDDP administration increased MDA levels and lipid peroxidation by 1.97- and 3.42-fold in the liver and kidney, respectively (Fig. 3). These findings are attributed to oxidative damage, which is interceded by the reproduction of MDA and a decrease in GSH levels (Abuzinadah and Ahmad, 2020; Fadl *et al*., 2020), via free radical formation that plays a vital role in CDDP-induced hepato-

Table 3. Total phenolic, total flavonoid, and antioxidant activity of HP.

`	Total phenolic (mg/GAC/g)	Total flavonoid (mg/RE/g)	DPPH scavenging activity (IC_{50} (µg/ml))
HP	121.56 ± 0.17	30.61 ± 0.08	96.2 ± 10

renal toxicity (Abdel-Razek *et al*., 2020; El-Shitany and Eid, 2017).

Treatment with HP extract (50 and 100 mg/kg) considerably improved the oxidative stress markers ($p < 0.05$) (Fig. 3). Moreover, 200 mg/kg of HP normalized these indicators (Fig. 3). A previous study reported that oral therapy with HP at 50 mg/kg reduced hepatic MDA content and improved oxidative stress (Bayramoglu *et al*., 2014). Importantly, HP extract significantly improved oxidative damage in liver and kidney tissues in a dose-dependent manner, possibly by increasing phenolic compounds in hepatic and renal cells, which have antioxidant effects (Izol *et al*., 2018).

Effect of HP on hepatic and renal inflammasome pathway

CDDP-induced hepato-renal toxicity has a multifactorial mechanism, of which the inflammatory response is an important one. Our findings demonstrate that CDDP can cause inflammation, as seen by a significant increment ($p < 0.05$) in all inflammatory markers, including TXNIP and NLRP3 contents (Fig. 4), along with cleaved caspase 1, NF-kβ, and IL-1β expressions (Fig. 5) in both hepatic and renal tissues, indicating that NLRP3 inflammasome assembly may be an important mechanism in triggering an inflammatory response in CDDP-induced acute liver and kidney injury in experiment animals (Ozkok *et al*., 2016; Molyvdas *et al*., 2018). These findings are compatible with a former study stating that activation of NLRP3 promotes caspase-1 cleavage, resulting in the generation of active IL-1β and increased cytokine secretion (Liu *et al*., 2018). In the current investigation, treatment with HP alone exhibited no significant effect on these parameters compared to normal mice. However, our findings revealed that the administration of HP could have anti-inflammatory effects by inhibiting NLRP3 inflammasome activation in a dose-dependent manner. Administration of HP (50 and 100 mg/kg) dramatically reduces hepatic and renal TXNIP and NLRP3 levels (Fig. 4), besides cleaved caspase 1, NF-kβ, and IL-1β expressions (Fig. 5). Meanwhile, 200 mg/kg HP possessed a superior effect, as it normalized all hepatic and renal inflammatory markers (Fig. 5). This modulating effect may be attributed to the HP compensatory technique against the inflammatory milieu produced in CDDP-treated mice. Our results were in convention with previous reports that have found an increase in proinflammatory cytokine expression, particularly IL-1β, in CDDP-induced hepatic and kidney injury (Molyvdas *et al*., 2018; Ozkok *et al*., 2016). Also, others have proved that the potent anti-inflammatory properties of HP are due to the bioactive constituents of HP (Novelli *et al*., 2014; Zhai *et al*., 2022).

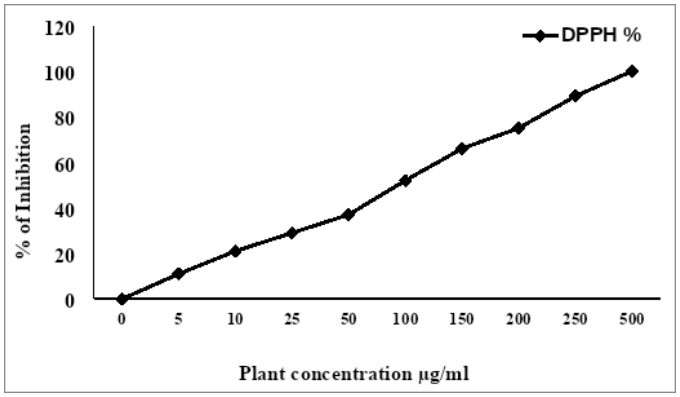

Figure 1. Inhibition percentage of HP.

Histopathological study

Liver sections from normal mice revealed normal hepatic lobular architecture with small portal tracts (Fig. 6A). CDDP-intoxicated mice revealed that several histological changes appear as hydropic degeneration, swelling hepatocytes, and widening of sinusoids (Fig. 6B). The liver section of CDDP-intoxicated mice treated with 50 mg/kg HP showed moderate hepatocytes degeneration, as well as a moderate widening of sinusoids (Fig. 6C). Furthermore, mice given 100 and 200 mg/kg HP had mostly normal hepatic lobular architecture (Fig. 6D and E). In line with these findings, CDDP-intoxicated mice had a significant degree of hepatic degeneration and inflammatory changes in the liver tissue (Tahoun *et al*., 2021).

Kidney sections from normal mice revealed typical cortical architecture, including normal renal glomeruli and tubules (Fig. 6F). The CDDP-intoxicated group exhibited significant histological abnormalities, including tubular epithelium degeneration and glomerular congestion (Fig. 6G). Moreover, 50 mg/kg HP-treated mice revealed focal thickening of Bowman's capsule with moderate degradation of the tubular epithelium (Fig. 6H). Yet, renal damage was ameliorated in 100 and 200 mg/

Table 4. Effect of HP on body weights and percentage of the organ to body weight ratios.

Animal Groups	Initial body weight	Final body weight	Kidney weight	Liver weight	Kidney-to-body weight ratio	Liver-to-body weight ratio
Normal	24.52 ± 1.40	26.03 ± 1.38	0.30 ± 0.04	1.17 ± 0.08	1.23 ± 0.12	4.80 ± 0.04
Normal HP (200 mg/kg)	22.92 ± 1.92	23.16 ± 1.86	0.21 ± 0.03	0.88 ± 0.15	0.95 ± 0.12	4.00 ± 0.59
CDDP	26.97 ± 3.89	21.63 ± 2.74	0.42 ± 0.07[a]	1.13 ± 0.19	2.00 ± 0.72[a]	5.51 ± 0.87[a]
HP + CDDP (50mg/kg)	24.07 ± 3.51	21.85 ± 3.17	0.23 ± 0.04[b]	0.84 ± 0.17	0.88 ± 0.25[b]	3.73 ± 1.42[b]
HP + CDDP (100mg/kg)	29.13 ± 1.94	27.43 ± 1.69	0.26 ± 0.11[b]	1.01 ± 0.17	1.03 ± 0.19[b]	3.73 ± 0.58[b]
HP + CDDP (200mg/kg)	23.70 ± 2.67	22.20 ± 2.23	0.21 ± 0.03[b]	0.86 ± 0.03	0.95 ± 0.25[b]	3.86 ± 0.60[b]

CDDP: Cisplatin; HP: *Hypericum perforatim*.
Values presented are means of six mice ± SEM. Statistical analysis was carried out using one-way ANOVA followed by LSD *post hoc* test.
[a, b] Significantly different from normal or CDDP groups at $p < 0.05$, respectively.

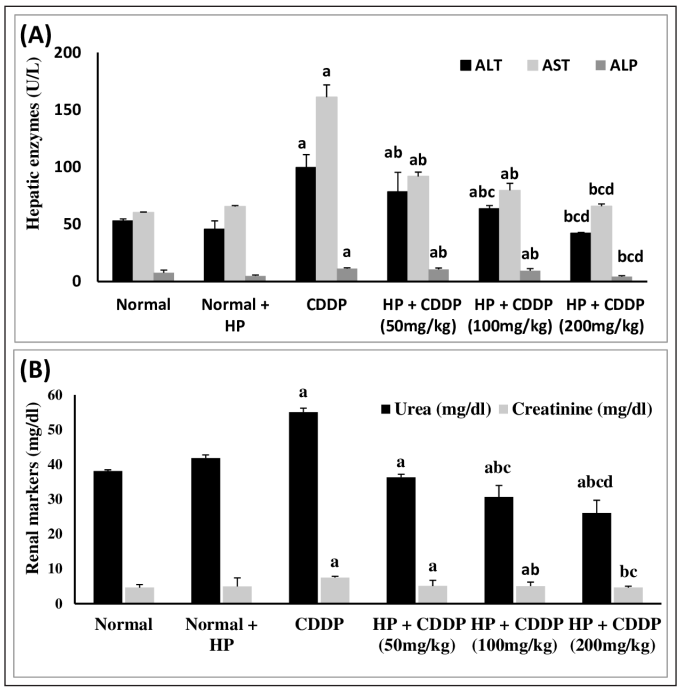

Figure 2. Effect of HP on (A) hepatic function (ALT, AST, and ALP) and (B) renal function markers (urea and creatinine). Values are presented as means of six mice ± SEM. Statistical analysis was carried out using one-way ANOVA followed by LSD *post hoc* test. [a–d] Significantly different from normal, CDDP, 50 mg/kg HP + CDDP or 100 mg/kg HP + CDDP groups at $p < 0.05$, respectively. ALT: alanine aminotransferase; AST: aspartate aminotransferase; ALP: alkaline phosphatase; CDDP:Cisplatin; HP: *Hypericum perforatum*.

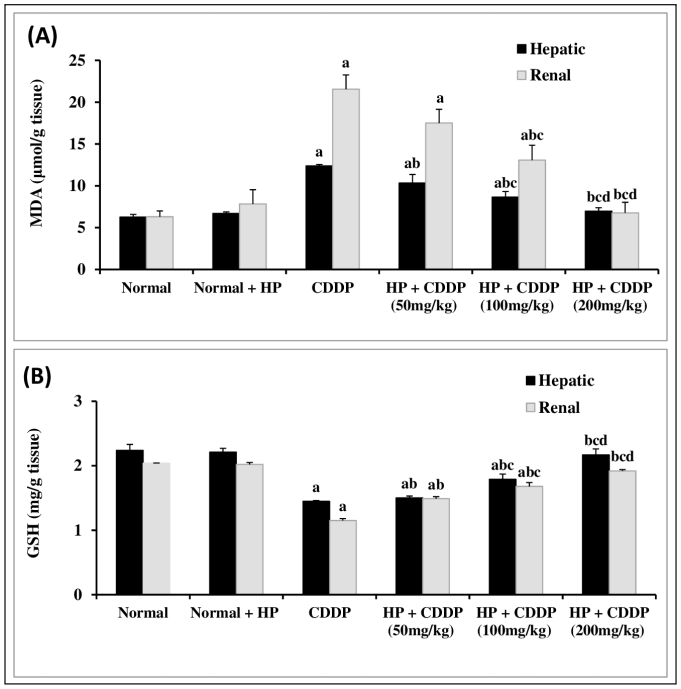

Figure 3. Effect of HP on hepatic and renal MDA (A) and GSH (B) contents. Values are presented as means of 6 mice ± SEM. Statistical analysis was carried out using one-way ANOVA followed by LSD *post hoc* test. [a, b, c,d] Significantly different from normal, CDDP, 50 mg/kg HP + CDDP or 100 mg/kg HP + CDDP at $p < 0.05$, respectively. CDDP: Cisplatin; HP: *Hypericum perforatum*, MDA: Malondialdehyde, GSH: reduced glutathione.

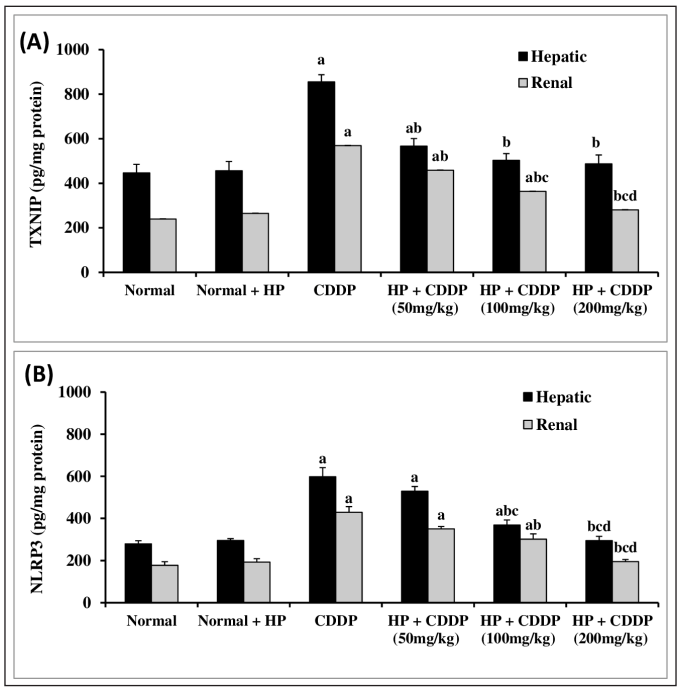

Figure 4. Effect of HP on hepatic and renal TXNIP (A) and NLRP3 (B) contents. Values are presented as means of 6 mice ± SEM. Statistical analysis was carried out using one-way ANOVA followed by LSD *post hoc* test. [a–d] Significantly different from normal, CDDP, 50 mg/kg HP + CDDP or 100 mg/kg HP + CDDP at $p < 0.05$, respectively. CDDP: Cisplatin; HP: *Hypericum perforatum,* TXNIP: Thioredoxin-interacting protein, NLRP3: NOD-like receptor pyrin domain-containing protein 3.

kg HP-treated mice by showing intact glomeruli and mild tubular epithelial degradation (Fig. 6I and J). Our results are consistent with those of others who observed the same CDDP-intoxicated mice's renal tissues (Elkomy *et al*., 2020). These findings confirmed the toxic effect of CDDP on hepatic and renal from both blood and tissue biochemical markers and inflammatory markers (Eweis *et al*., 2020). Furthermore, these results established the promising effect of HP in enhancing all injuries induced by CDDP.

HPLC fingerprinting analyses

Our findings revealed that HP methanol extract contains many phenolic and flavonoid components. The methanol extract was compared to thirteen standard phenolic acids and eight standard flavonoids (Tables 5 and 6; Figs. 7 and 8) using HPLC fingerprinting analyses to identify the relative proportions of these compounds in the extract.

The most prevalent phenolic acids found were ellagic acid and cinnamic acid (10.95 and 8.36 g/ml, respectively). Minor components were catechol, caffeic acid, gallic acid, and syringic acid (3.22, 2.46, 2.14, and 1.14 g/ml, respectively). The extract did not include chlorogenic acid, p-coumaric acid, protocatechuic acid, ferulic acid, or salicylic acid. Instead, the main flavonoids in the extract were quercetin and hesperidin (12.39 and 11.69 g/ml, respectively). On the contrary, catechin, naringin, luteolin, and kaempferol were found as minor components (4.35, 4.22, 3.18, and 2.49 g/ml, respectively). However, the extract missed 7-OH flavone and rutin. These results are consistent with those of previous literature (Sarikurkcu *et al*., 2020; Zou *et al*., 2004).

Particularly, this study differs from previous HP investigations in the absence of rutin, chlorogenic, p-coumaric, and protocatechuic acids (Sarikurkcu *et al*., 2020).

Phenolic acids and flavonoids are two types of phenolic chemicals that have the strongest antioxidant activity in treating oxidative stress and related issues such as inflammation and hepato-renal disease with the least amount of side effects (Abdel-Hady *et al*., 2018). According to previous research, ellagic and cinnamic acid (pure phenolic acids) provided a significant protective effect against CDDP-induced hepatotoxicity and nephrotoxicity because of their anti-inflammatory and free radical scavenging activities (Tohamy *et al*., 2016). These compounds

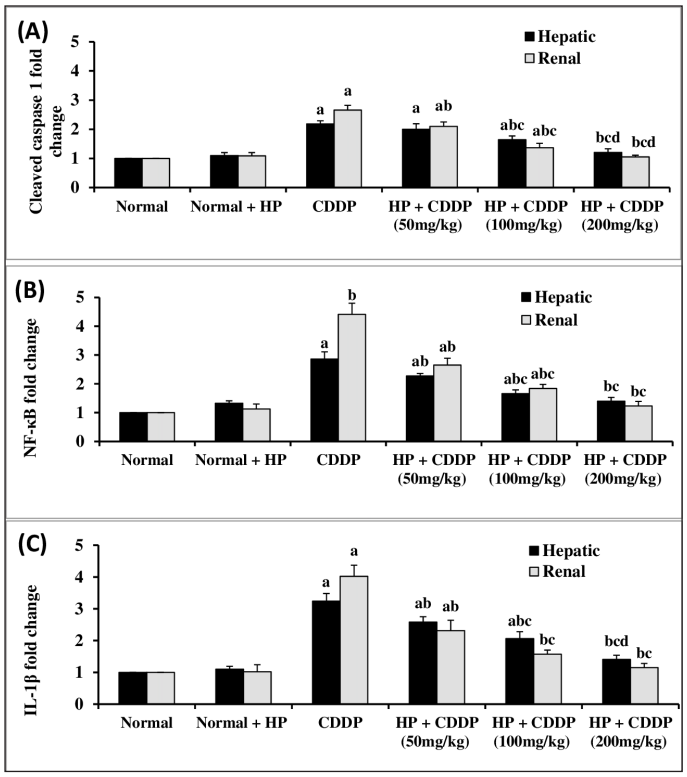

Figure 5. Effect of HP on hepatic and renal cleaved caspase 1 (A), NF-kβ (B), and IL-1β (C) expressions. Values are presented as means of 6 mice ± SEM. Statistical analysis was carried out using one-way ANOVA followed by LSD *post hoc* test. [a–d] Significantly different from normal, CDDP, 50 mg/kg HP + CDDP or 100 mg/kg HP + CDDP at $p < 0.05$, respectively. CDDP: Cisplatin; HP: *Hypericum perforatum,* NF-kβ: nuclear factor kappa-β, IL-1β: Interleukin-1β.

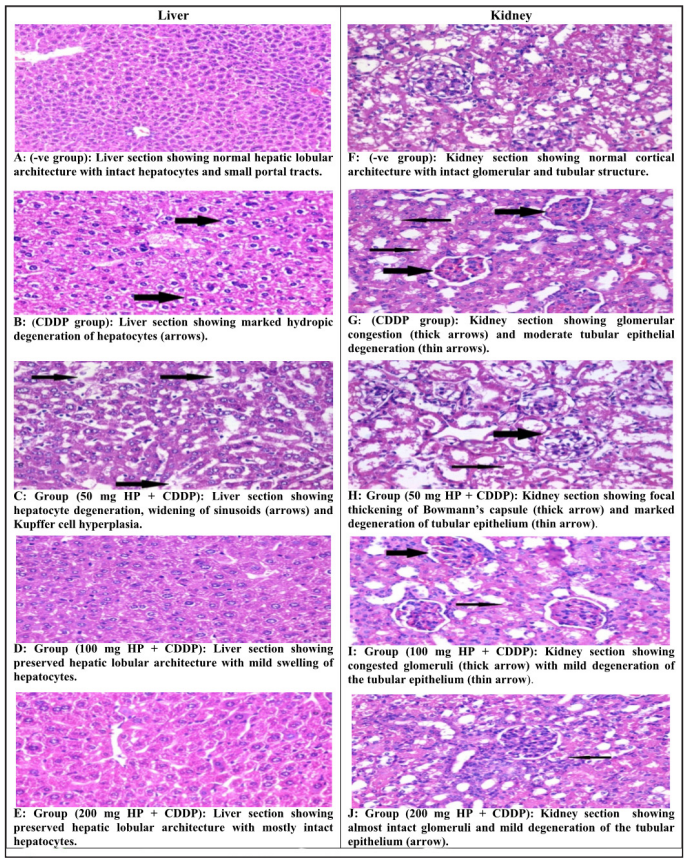

Figure 6. (A–J) Effect of different doses of HP on histopathological changes in liver and kidney tissues in CDDP-intoxicated mice (H&E Stain, ×400).

Table 5. Phenolic acid concentrations in HP MeOH extract compared to 13 phenolic acid standards.

Compounds	Rt	Standards Concentration µg/ml	MeOH extract Concentration µg/ml
Chlorogenic acid	3.0	7.88	--
Catechol	4.0	3.45	3.22
Syringenic acid	5.0	3.56	1.14
p-coumaric acid	6.0	10.14	--
Cinnamic acid	7.0	9.79	8.36
Caffeic acid	8.0	3.69	2.46
Pyrogallol	9.0	9.77	0.69
Gallic acid	10.0	2.56	2.14
Protocatechuic acid	10.5	2.31	--
Ferulic acid	11.0	11.09	--
Salicylic acid	12.0	2.17	--
Ellagic acid	13.5	3.09	10.95
Benzoic acid	15	4.19	0.97

Table 6. Flavonoid concentrations in HP MeOH extract compared to eight flavonoid compound standards.

Compounds	Rt	Standards Concentration µg/ml	MeOH extract Concentration µg/ml
7-OH flavone	3.0	5.22	--
Naringin	4.0	9.06	4.22
Rutin	5.0	6.14	--
Quercetin	7.0	3.04	12.39
Kaempferol	8.0	4.16	2.49
Luteolin	9.0	10.22	3.18
Hesperidin	10.0	3.88	11.69
Catechin	12.0	4.39	4.35

markedly reduced creatinine and urea levels, counteracted the damaging effects of CDDP on redox imbalance markers, and improved histopathological changes (Goyal *et al*., 2019; Tohamy *et al*., 2016). Quercetin and hesperidin have antioxidant properties and could improve hepato-renal dysfunctions and protect against CDDP by lowering serum ALT, AST, creatinine, and urea levels. Furthermore, they decrease oxidative damage by considerably reducing MDA and increasing GSH content in liver and kidney tissues, resulting in the relief of histological abnormalities (Aboraya *et al*., 2022). Moreover, the minor phenolic compounds have antioxidant and anti-inflammatory properties due to their free radical scavenging potential as a result of their structure and modes of action (Veiko *et al*., 2021). All of these data point to the fact that HP MeOH extract could assist in minimizing hepato-renal inflammation and oxidative stress.

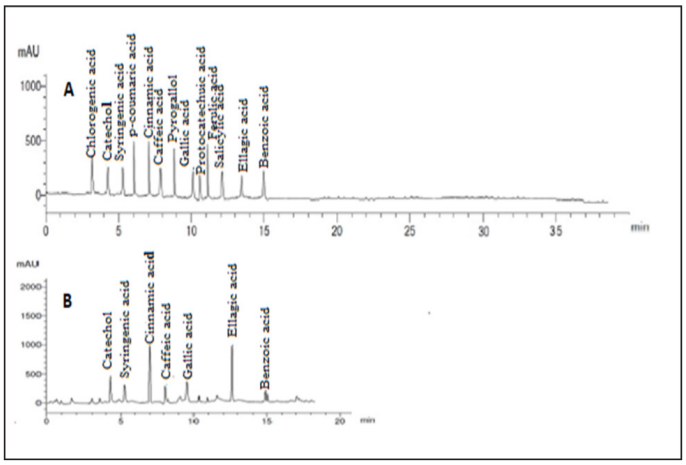

Figure 7. HPLC-fingerprint chromatogram of (A) eight standard phenolic acid compounds and (B) MeOH extract of HP.

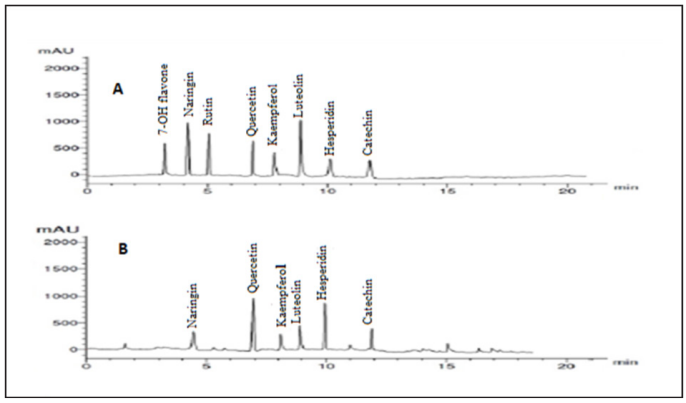

Figure 8. HPLC-fingerprint chromatogram of (A) eight standard flavonoid compounds and (B) MeOH extract of HP.

Table 7. Chemical composition of the MeOH extract of HP identified by GC-MS.

No.	RT (minute)	MF	MW	Name	Area Sum%
1	3.49	$C_5H_{10}O_3$	118	β-hydroxyisovaleric acid (β-Hydroxy β-methylbutyric acid)	28.89
2	3.93	$C_9H_{10}O_2$	150	Hydrocinnamic acid	2.77
3	5.32	$C_{14}H_{22}O_2$	222	3,5 di-t-Butyl catechol	0.66
4	5.84	$C_8H_5N_3O_2S$	207	4-[4-nitrophenyl]- 1,2,3 thiadiazole	1.4
5	7.49	$C_{17}H_{14}O_4$	282	5-Hydroxy-7-methoxy-2-methyl-3-phenyl-4-chromenone	1.42
6	8.48	$C_{17}H_{14}O_5$	298	3-Hydroxy-7-methoxy-2-(4-methoxyphenyl)-4H-chromen-4-one	2.83
7	10.25	$C_{17}H_{14}O_5$	298	Coumarin, 3-(3,4 dimethoxyphenyl)	0.48
8	10.95	$C_7H_9N_7O_2$	223	3,7 diacetamido-7H-S-triazolo[5,1-C]-S-triazole	3.18
9	11.97	$C_{27}H_{44}O_3$	416	24,25-Dihydroxy vitamin D3	3.24
10	13	$C_{15}H_{24}$	204	B-Guaiene	1.21
11	13.19	$C_{15}H_{24}$	204	γ- Himachalene	3.67
12	13.82	$C_{15}H_{24}O_2$	236	Corymbolone	1.44
13	15.05	$C_{18}H_{36}O_2$	284	Hexadecanoic acid, 14-methyl, methyl ester	1.87
14	15.91	$C_{23}H_{42}O_2$	350	Methyl 5,13-docosadienoate	0.8
15	16.23	$C_{19}H_{34}O_2$	294	Methyl cis-9, cis-15-linoleate	0.57
16	16.58	$C_{17}H_{34}O_2$	270	Hexadecanoic acid, methyl ester (Methyl palmitate)	31.89
17	17.04	$C_{36}H_{60}O_2$	524	Vitamin A palmitate	3.19
18	17.33	$C_{24}H_{42}O_7$	442	L-Ascorbic acid, 6-stearate	1.68
19	17.87	$C_{18}H_{30}O_2$	280	Linolenic acid	6.04
20	18.02	$C_{19}H_{38}O_2$	298	Methyl stearate	2.78

GC-MS analysis

According to our findings, MeOH extract contains a wide variety of bioactive components and has the highest bioactivities. It was analyzed using GC-MS in order to identify the phytochemicals responsible for its action (Table 7, Fig. 9). In the MeOH extract of HP, 20 compounds were identified, accounting for about 100.10% of the total peak area. Hexadecanoic acid, methyl ester (methyl palmitate), was the most abundant compound (31.89%), followed by β-hydroxyisovaleric acid (28.89%), linolenic acid (6.04%), γ-himachalene (3.67%), 3,7-diacetamido-7H-S-triazolo[5, 1-C]-S-triazole (3.18%), 24,25-dihydroxy vitamin D3 (3.24%), and vitamin A palmitate (3.19%).

Methyl palmitate, known as fatty acid, has antioxidant, anti-inflammatory, and hepatoprotective activity. It was reported as the minor compound of Turkish *Hypericum uniglandulosum* and *Hypericum salsugineum* (Özkan *et al*., 2011). β-Hydroxyisovaleric acid is a derivative of the amino acid leucine. It is thought to improve liver function because it is naturally produced in the human liver (Holeček and Vodeničarovová, 2018). β-Hydroxyisovaleric acid was found in HP grown in Saudi Arabia for the first time via GC-MS analysis (Bagdonaite *et al*., 2012). Linolenic acid (6.04%) is an omega-3 fatty acid with anti-inflammatory and anti-fibrotic activities that improve liver function. Depending on the plant's origin, linolenic acid has been identified as the most plentiful fatty acid in the *Hypericum* species (Hosni *et al*., 2017). γ-Himachalene is a sesquiterpene known to be immune system supportive in terms of acting as an antioxidant and anti-inflammatory agent and aiding in cellular repair (Taleb *et al*., 2016). Himachalene isomers were reported in the *Hypericum* species (Cirak *et al*., 2022; Jaimand *et al*., 2012). Therefore, the effective anti-inflammatory activity of the PH could be attributed to the presence of a high concentration of specific compounds with anti-inflammatory activity.

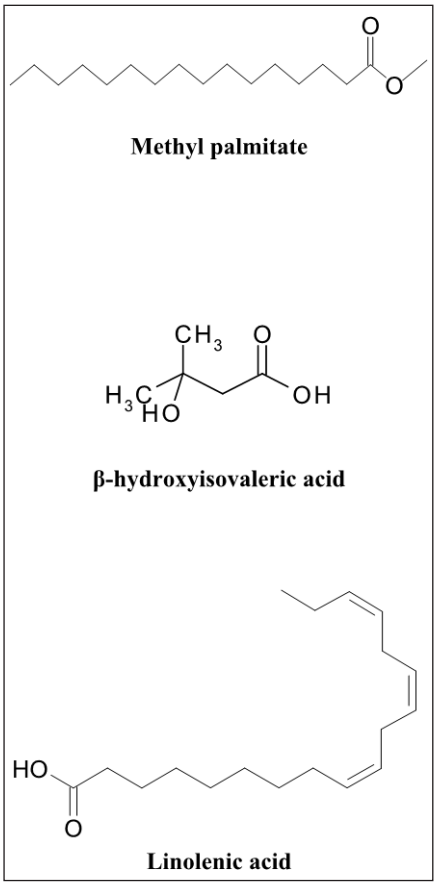

Figure 9. Structure of the major compounds identified by GC-MS of HP.

CONCLUSION

HP protects against hepato-renal injuries induced by CDDP in terms of dose-dependent improvements in all examined biomarkers, with the most significant effect achieved at 200 mg/kg. Furthermore, these benefits are at least partially achieved by inhibiting the activation of the TXNIP/NLRP3 inflammasome pathway. HP protective action could be related to its phytochemical profile, specifically ellagic acid, cinnamic acid, quercetin, and hesperidin. So, the administration of HP as an adjuvant therapy with CDDP for cancer treatment could be a viable approach.

AUTHOR CONTRIBUTION

Maha B. Salem was responsible for the experimental design, investigation of RT-PCR, oxidative stress and ELISA analysis, data acquisition, statistical analysis, data interpretation, and writing the original draft. Eman A. Morsi was responsible for the characterization of compounds conducted on the database library, data analysis, preparation of figures, data curation, and writing the original draft. Eman A. El-Wakil was responsible for the selection and collection of the plant, preparation of extract, conceptualization, and supervision. Naglaa M. El-Lakkany was responsible for the conceptualization, validation, data curation, formal analysis, and reviewing and editing of the manuscript. Tarek Abou-Shousha was responsible for the investigation of the histological study. Heba Abdel-Hady was responsible for the experimental design, investigation of phytochemical screening, antioxidant assay, biomarkers analysis, data acquisition, statistical analysis, and writing of the original draft. All authors revised and read the manuscript. All of them approved the manuscript for publication

FINANCIAL SUPPORT

This research did not receive any support or grants from any financial organization.

CONFLICTS OF INTEREST

The authors report no financial or any other conflicts of interest in this work.

ETHICAL APPROVALS

The study was permitted by the TBRI Ethical Committee (PT 613, 28 June 2021; FWA 0010609).

DATA AVAILABILITY

All generated and analyzed data are included in the article.

PUBLISHER'S NOTE

This journal remains neutral with regard to jurisdictional claims in published institutional affiliation.

REFERENCES

Abdel-Hady H, El-Sayed MM, Abdel-Hady AA, Hashash MM, Abdel-Hady AM, Aboushousha T, Abdel-Hameed ES, Abdel-Lateef EE, Morsi EA. Nephroprotective activity of methanolic extract of *Lantana camara* and squash (*Cucurbita pepo*) on cisplatin-induced nephrotoxicity in rats and identification of certain chemical constituents of *Lantana camara* by HPLC-ESI-MS. Pharmacog J, 2018; 10(1):136–47.

Abdel-Hady H, El-Wakil EA, Abdel-Gawad M. GC-MS analysis, antioxidant and cytotoxic activities of *Mentha spicata*. Euro J Med Plants, 2018; 26(1):1–2.

Abdel-Razek EA, Abo-Youssef AM, Azouz AA. Benzbromarone mitigates cisplatin nephrotoxicity involving enhanced peroxisome proliferator-activated receptor-alpha (PPAR-α) expression. Life Sci, 2020; 243:117272.

Abo-Elmaaty A, Behairy A, El-Naseery NI, Abdel-Daim MM. The protective efficacy of vitamin E and cod liver oil against cisplatin-induced acute kidney injury in rats. Environ Sci Poll Res, 2020; 27(35):44412–26.

Aboraya DM, El Baz A, Risha EF, Abdelhamid FM. Hesperidin ameliorates cisplatin induced hepatotoxicity and attenuates oxidative damage, cell apoptosis, and inflammation in rats. Saudi J Bio Sci, 2022; 29(5):3157–66.

Abuzinadah MF, Ahmad A. Pharmacological studies on the efficacy of a thymoquinone-containing novel polyherbal formulation against cisplatin-induced hepatorenal toxicity in rats. J Food Biochem, 2020; 51:113–21.

Adejor EB, Ameh DA, James DB, Owolabi OA, Ndidi US. Effects of *Garcinia kola* biflavonoid fractions on serum lipid profile and kidney function parameters in hyperlipidemic rats. Clin Phytosci, 2017; 2(1):1–8.

Anders HJ, Muruve DA. The inflammasomes in kidney disease. J Am Soc Nephrol, 2011; 22(6):1007–8.

Aranda-Rivera AK, Srivastava A, Cruz-Gregorio A, Pedraza-Chaverri J, Mulay SR, Scholze A. Involvement of inflammasome components in kidney disease. Antioxid, 2022; 27(11):2–46.

Arokiyaraj S, Balamurugan R, Augustian P. Antihyperglycemic effect of *Hypericum perforatum* ethyl acetate extract on streptozotocin–induced diabetic rats. Asian Pac J Trop Biomed, 2011; 1(5): 386–90.

Asgharian A, Ojani S. *In vitro* antioxidant activity and phytochemical screening of flowers and leaves of *Hypericum perforatum* L. ethanolic extracts from Tonekabon-Iran. J Phytochem Biochem, 2017; 1:1–5.

Bagdonaite E, Janulis V, Ivanauskas L, Labokas J. Between species diversity of *Hypericum perforatum* and *H. maculatum* by the content of bioactive compounds. Nat Prod Commun, 2012; 7(2):199–200.

Bayramoglu G, Bayramoglu A, Engur S, Senturk H, Ozturk N, Colak S. The hepatoprotective effects of *Hypericum perforatum* L. on hepatic ischemia/reperfusion injury in rats. Cytotechnol, 2014; 66(3):443–8.

Brand-Williams W, Cuvelier ME, Berset CL. Use of a free radical method to evaluate antioxidant activity. LWT-Food Sci Tech, 1995; 28(1):25–30.

Caglar HG, Selek S, Koktasoglu F, Koyuncu I, Demirel M, Sarikaya A, Meydan S. Effect of *Camellia sinensis*, *Hypericum perforatum* and *Urtica dioica* on kidney and liver injury induced by carbon tetrachloride in rats. Cell Mol Biol, 2019; 65(5):79–86.

Cirak C, Seyis F, Özcan A, Yurteri E. Ontogenetic changes in phenolic contents and volatile composition of *Hypericum androsaemum* and *Hypericum xylosteifolium*. Biochem Systematics Ecol, 2022; 1(102):104429.

Dasari S, Tchounwou PB. Cisplatin in cancer therapy: molecular mechanisms of action. Europ J Pharmacol, 2014; 5(740):364–78.

Domitrović, R., Cvijanović, O., Pernjak-Pugel, E., Škoda, M., Mikelić, L. and Crnčević-Orlić, Ž. Berberine exerts nephroprotective effect against cisplatin-induced kidney damage through inhibition of oxidative/nitrosative stress, inflammation, autophagy and apoptosis. Food Chem Tox, 2013; 62:397–406.

El-Hawary SS, Ibrahim RM, Hamed AR, El-Halawany AM. Nutritional evaluation, chemical investigation of phenolic content and antioxidant activity of *Ferocactus glaucescens* ripe fruits. Egy J Chem, 2020; 63(7):2435–44.

Elkomy A, Abdelhiee EY, Fadl SE, Emam MA, Gad FA, Sallam A, Alarifi S, Abdel-Daim MM, Aboubakr M. L-carnitine mitigates oxidative stress and disorganization of cytoskeleton intermediate filaments in cisplatin-induced hepato-renal toxicity in rats. Front Pharm, 2020; 11:574441.

Elsayed A, Elkomy A, Elkammar R, Youssef G, Abdelhiee EY, Abdo W, Fadl SE, Soliman A, Aboubakr M. Synergistic protective effects of lycopene and N-acetylcysteine against cisplatin-induced hepatorenal toxicity in rats. Sci Rep, 2021; 11(1):1–0.

El-Shitany NA, Eid B. Proanthocyanidin protects against cisplatin-induced oxidative liver damage through inhibition of inflammation and NF-κβ/TLR-4 pathway. Environ Toxicol, 2017; 32(7):1952–63.

El-Wakil EA, Morsi EA, Abel-Hady H. Phytochemical screening, antimicrobial evaluation and GC-MS analysis of cyperus rotundus. World J Pharm Pharm Sci, 2019; 8(9):129–39.

Ersoy E, Ozkan EE, Boga M, Mat A. Evaluation of *in vitro* biological activities of three Hypericum species (*H. calycinum*, *H. confertum*, and *H. perforatum*) from Turkey. South Afri J Botany, 2020; 1(130):141–7.

Eweis HS, Bashraf OM, Ali AS, Ali SS. Antioxidant traits and protective impact of vorinostat against cisplatin induced hepatoxicity in rats. J Pharm Res Int, 2020; 32:58–73.

Fadl SE, El-Shenawy AM, Gad DM, El Daysty EM, El-Sheshtawy HS, Abdo WS. Trial for reduction of Ochratoxin A residues in fish feed by using nano particles of hydrated sodium aluminum silicates (NPsHSCAS) and copper oxide. Toxicon, 2020; 184:1–9.

Farid AS, El Shemy MA, Nafie E, Hegazy AM, Abdelhiee EY. Anti-inflammatory, anti-oxidant and hepatoprotective effects of lactoferrin in rats. Drug Chem Tox, 2021; 44(3):286–93.

Goyal Y, Koul A, Ranawat P. Ellagic acid ameliorates cisplatin induced hepatotoxicity in colon carcinogenesis. Environ Toxicol, 2019; 34(7):804–13.

Greeson JM, Sanford B, Monti DA. St. John's wort (*Hypericum perforatum*): a review of the current pharmacological, toxicological, and clinical literature. Psychopharmacol, 2001; 153(4):402–14.

Güzel A, Akyüz M, Sanda MA. Determination of antioxidant activity of *Hypericum perforatum*. Bütünleyici Anadolu Tıbbı Derg, 2019;1(1):9–18.

Hady HA, El wakil EA, Nasr SM. Characterization and evaluation of antimicrobial and cytotoxic activities of glycine max methanol extract. Inter J Pharm Res, 2019; 11(2):418–26.

Holeček M, Vodeničarovová M. Effects of beta-hydroxy-beta-methylbutyrate in partially hepatectomized rats. Physiol Res, 2018; 67(5):741–51.

Hosni K, Msaâda K, Taârit MB, Marzouk B. Fatty acid composition and tocopherol content in four Tunisian *Hypericum* species: *Hypericum perforatum*, *Hypericum tomentosum*, *Hypericum perfoliatum* and *Hypericum ericoides* ssp. Roberti. Arab J Chem, 2017; 10:S2736–41.

Izol V, Arıdoğan IA, Tansuğ Z, Doran F, Erdoğan KE, Kaplan HM, Şİngİrİk E, Ertuğ P, Pazarci P. *Hypericum perforatum* extract against oxidative stress, apoptosis and oedema in kidney induced by gentamicin. Inter J Pharm, 2019; 15(1):66–73.

Jaimand K, Rezaee MB, Naderi M, Mozaffrian V, Azadi R, Karimi S, Gholipoor M. Chemical composition of the essential oils of six *Hypericum* species (Hypericaceae) from Iran. J Med Plants By Prod, 2012; 1(1):7–11.

Kim ES, Lee JS, Akram M, Kim KA, Shin YJ, Yu JH, Bae ON. Protective activity of *Dendropanax morbifera* against cisplatin-induced acute kidney injury. Kidney Blood Pressure Res, 2015; 40(1):1–2.

Kumar A, Garg R, Prakash AK. Effect of St. John's Wort (*Hypericum perforatum*) treatment on restraint stress-induced behavioral and biochemical alteration in mice. BMC Comp Alter Med, 2010; 10(1):1–6.

Kuntić V, Pejić N, Ivković B, Vujić Z, Ilić K, Mićić S, Vukojević V. Isocratic RP-HPLC method for rutin determination in solid oral dosage forms. J Pharm Biomed Anal, 2007; 43(2):718–21.

Lin MT, Ko JL, Liu TC, Chao PT, Ou CC. Protective effect of D-methionine on body weight loss, anorexia, and nephrotoxicity in cisplatin-induced chronic toxicity in rats. Integr Cancer Ther, 2018; 17(3):813–24.

Lin YL, Juan IM, Chen YL, Liang YC, Lin JK. Composition of polyphenols in fresh tea leaves and associations of their oxygen-radical-absorbing capacity with antiproliferative actions in fibroblast cells. J Agri Food Chem, 1996; 44(6):1387–94.

Liu Q, Zhang D, Hu D, Zhou X, Zhou Y. The role of mitochondria in NLRP3 inflammasome activation. Mol Immun, 2018; 103:115–24.

Livak KJ, Schmittgen TD. Analysis of relative gene expression data using real-time quantitative PCR and the $2^{-\Delta\Delta CT}$ method. Methods, 2001; 25(4):402–8.

Lowry OH. Protein measurement with the folin phenol reagent. J biol Chem, 1951;193:265–75.

Mašković PZ, Mladenović JD, Cvijović MS, Aćamović-Đoković G, Solujić SR, Radojković MM. Phenolic content, antioxidant and antifungal activities of acetonic, ethanolic and petroleum ether extracts of *Hypericum perforatum* L. Hemijska Ind, 2011; 65(2):159–64.

Molyvdas A, Georgopoulou U, Lazaridis N, Hytiroglou P, Dimitriadis A, Foka P, Vassiliadis T, Loli G, Phillipidis A, Zebekakis P, Germenis AE. The role of the NLRP3 inflammasome and the activation of IL-1β in the pathogenesis of chronic viral hepatic inflammation. Cytokine, 2018; 1(110):389–96.

Napoli E, Siracusa L, Ruberto G, Carrubba A, Lazzara S, Speciale A, Cimino F, Saija A, Cristani M. Phytochemical profiles, phototoxic and antioxidant properties of eleven *Hypericum* species—a comparative study. Phytochem, 2018; 152:162–73.

Negi JS, Singh P, Rawat B. Chemical constituents and biological importance of Swertia: a review. Curr Res Chem, 2011; 3(1):1–5.

Novelli M, Beffy P, Menegazzi M, De Tata V, Martino L, Sgarbossa A, Porozov S, Pippa A, Masini M, Marchetti P, Masiello P. St. John's wort extract and hyperforin protect rat and human pancreatic islets against cytokine toxicity. Acta Diabetol, 2014; 51(1):113–21.

Özkan EE, Gürer ÇÜ, Kültür Ş, Mat A. Quantitative and qualitative studies on five endemic *Hypericum* species of Turkey. Planta Med, 2011; 77(12):PL96.

Ozkok A, Ravichandran K, Wang Q, Ljubanovic D, Edelstein CL. NF-κB transcriptional inhibition ameliorates cisplatin-induced acute kidney injury (AKI). Toxicol Lett, 2016; 240(1):105–13.

Pardo-de-Santayana M, Quave CL, Sõukand R, Pieroni A. Medical ethnobotany and ethnopharmacology of Europe. Ethnopharmacology, 2015; 18:343–56.

Rashid A, Waseem N, Younus N, Adnan N, Faisal L. Histomorphological effects of *Withania somnifera* root extract against cisplatin induced renal lesions in rats. Pak J Med Health Sci, 2021; 15(2):235–9.

Sallam AO, Rizk HA, Emam MA, Fadl SE, Abdelhiee EY, Khater H, Elkomy A, Aboubakr M. The ameliorative effects of L-Carnitine against Cisplatin-induced Gonadal toxicity in rats. Pak Vet J, 2021; 41(1):147–51.

Sarikurkcu C, Locatelli M, Tartaglia A, Ferrone V, Juszczak AM, Ozer MS, Tepe B, Tomczyk M. Enzyme and biological activities of the water extracts from the plants *Aesculus hippocastanum*, *Olea europaea* and *Hypericum perforatum* that are used as folk remedies in Turkey. Molecules, 2020; 25(5):1202.

Siangu BN, Swaleh S, Mwonjoria KJ, Wilson MN. Antioxidant activity, total phenolic and flavonoid content of selected Kenyan medicinal plants, sea algae and medicinal wild mushrooms. Afr J Pure Appl Chem, 2019; 13(3):43–8.

Singleton VL, Orthofer R, Lamuela-Raventós RM. Analysis of total phenols and other oxidation substrates and antioxidants by means of folin-ciocalteu reagent. Methods Enzymol, 1999; 299:152–78.

Sioud F, Mangelinckx S, Lahmer A, Bonneure E, Chaabene F. Alkaloids isolated from ephedra alata: characterization and protective effects against cisplatin-induced liver and kidney injuries in mice. Biomed J Sci Tech Res, 2021; 36(3):28591–602.

Sologub V, Grytsyk A. The research of the hypericum extract's pharmacological activity. Pharm Innov, 2013; 1(11, Part A):85.

Tahoun E, Elgedawy G, El-Bahrawy A. Cytoprotective effect of ginger extract on cisplatin-induced hepatorenal toxicity in rats via modulation of oxidative stress, inflammation and apoptosis: histopathological, biochemical and immunohistochemical study. Com Clin Path, 2021; 30(4):647–3.

Taleb RI, Najm P, Shebaby W, Boulos JC, Demirdjian S, Hariri E, El-Sibai M, Daher C, Mroueh M. β-2-himachalen-6-ol: a novel anticancer sesquiterpene unique to the lebanese wild carrot. J Ethnopharmacol, 2016; 190:59–67.

Tohamy AA, Aref AM, Abdel Moneim AE, Sayed RH. Cinnamic acid attenuates cisplatin-induced hepatotoxicity and nephrotoxicity. J Basic Environ Sci, 2016; 3:1–9.

Veiko AG, Lapshina EA, Zavodnik IB. Comparative analysis of molecular properties and reactions with oxidants for quercetin, catechin, and naringenin. Mol Cell Biochem, 2021; 476(12):4287–99.

Victor BK, Shaikh Hamed WMA. Preliminary phytochemical screening and evaluation of *in vitro* antioxidant activity of iraqi species of *Hypericum perforatum* aerial part. Int Res J Pharm, 2014; 5:369–73.

Wu M, Han W, Song S, Du Y, Liu C, Chen N, Wu H, Shi Y, Duan H. NLRP3 deficiency ameliorates renal inflammation and fibrosis in diabetic mice. Mol Cell Endocrinol, 2018; 15(478):115–25.

Yadav M, Chatterji S, Gupta SK, Watal G. Preliminary phytochemical screening of six medicinal plants used in traditional medicine. Int J Pharm Pharm Sci, 2014; 6(5):539–42.

Zhai X, Chen Y, Han X, Zhu Y, Li X, Zhang Y, Lu Y. The protective effect of hypericin on postpartum depression rat model by inhibiting the NLRP3 inflammasome activation and regulating glucocorticoid metabolism. Int Immunopharmacol, 2022; 1(105):108560.

Zhishen J, Mengcheng T, Jianming W. The determination of flavonoid contents in mulberry and their scavenging effects on superoxide radicals. Food Chem, 1999; 64(4):555–9.

Zou Y, Lu Y, Wei D. Antioxidant activity of a flavonoid-rich extract of *Hypericum perforatum* L. *in vitro*. J Agr Food Chem, 2004; 52(16):5032–9.

How to cite this article:
Salem MB, Morsi EA, El-Wakil EA, El-Lakkany NM, Abou-shousha T, Abdel-Hady H. HPLC fingerprinting/GC-MS analysis, and efficacy of *Hypericum perforatum* against cisplatin-induced hepato-renal toxicity in mice with insights into the TXNIP/NLRP3 pathway. J Appl Pharm Sci, 2023; 13(09):037–047.